Charge splitting among anodes of a CdZnTe strip detector

E. Kalemci[a], J. L. Matteson[a]

[a]Center for Astrophysics and Space Sciences, University of California
San Diego
9500 Gilman Dr., La Jolla, CA 92093-0424

ABSTRACT

We have studied charge splitting among the anodes of a CdZnTe (CZT) strip detector using a 30 μm collimated X-ray beam. The results indicate that charge splitting is a consequence of photoelectron range and diffusion. We also studied charge loss to the inter-anode regions. We showed that the charge loss increases as depth of interaction increases for interactions occurring above the inter-anode region.

Keywords: CdZnTe, CZT detectors, strip detectors, solid state detectors, X-ray astronomy, diffusion

1. INTRODUCTION

We have developed and tested position-sensitive cross-strip CZT detectors for use in X-ray astronomy in collaboration with Washington University in St. Louis.[1–3] For the results presented here, we used the UCSD-WU detector (see Fig. 1), which is configured with 22 anode strips on one side and 22 orthogonal cathode strips on the other side. A set of steering electrodes is interlaced with the anodes to enhance charge collection. Anodes and steering electrodes are 100 μm wide while cathodes are 450 μm. Anodes are biased at 200 V and the steering electrode is biased at 180 V. The pitch is 500 μm. X-rays are incident are incident on the detector's cathode side.

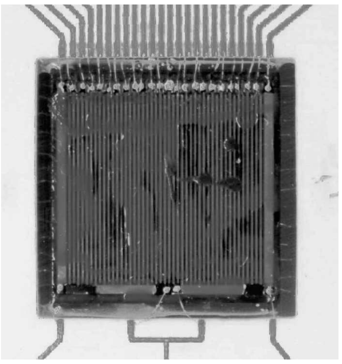

Figure 1. Prototype CZT strip detector. 22 anode strips with 500 microns pitch and 22 steering electrodes. Total size is 12x12x2 mm^3.

Previously, we modeled charge drift in the detector and charge induction on the electrodes as a function of time.[1] It took charge trapping into account and determined the signal induced on electrodes using Ramo's weighting potential method.[4] The electric field calculation was performed by the commercial program MAXWELL[5] with the result shown in Fig. 2. This "non-diffusive" work modeled the ideal case where each interaction occurred at a point, with no lateral expansion of the charge cloud. In this case the electrons and holes followed single electric field lines to single electrodes. In reality, there are additional effects which broaden the distribution of charges and produce charge splitting between electrodes. Here, we study a more accurate model which includes effects such as diffusion and photoelectron range.

Charge splitting can limit the performance of multi-electrode detectors. Depending on the distance between electrodes and the potential distribution in the detector, some of the electrons might drift to inter-anode regions and cause incomplete charge collection. Moreover, the size of the charge splitting region may limit the achievable spatial resolution. We studied charge splitting by measuring the size of electron diffusion cloud and the amount of electron charge loss versus interaction position in the detector. These results were compared with the predictions of our charge collection model.

We used a collimated X-ray beam to scan across the electrodes of the prototype cross-strip CZT detector and analyzed the observed pulse heights. A more detailed report on this study has been submitted to elsewhere.[6] Similar studies have been done by other groups with pixel detectors. Du et al.[7] and He et al.[8] investigated charge splitting in 3-D position sensitive CdZnTe spectrometers and obtained estimates of electron cloud sizes for different gamma-ray sources. Bolotnikov et al.[9] studied the charge loss to inter-pixel gaps. Prettyman et al.[10] examined the charge splitting effect on coplanar grid detectors and investigated gap events.

Further author information:
E. Kalemci: E-mail: emrahk@mamacass.ucsd.edu

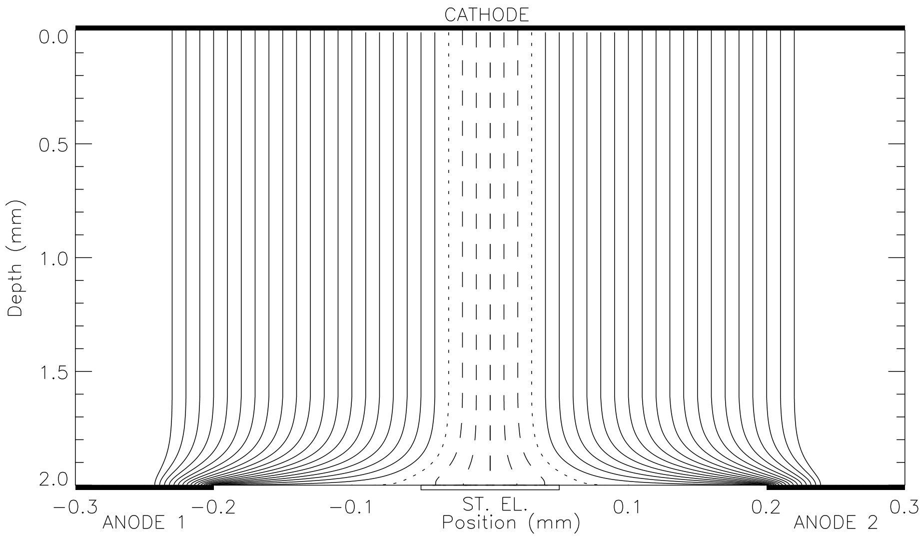

Figure 2. Model calculation of charge drift trajectories. (X- and y-axes are not scaled the same.) Filled boxes are anodes and the empty box is the steering electrode. Solid lines terminate at anodes, dashed lines terminate at steering electrode and dotted lines terminate in the gap between.

2. PHOTOELECTRON RANGE AND DIFFUSION

A photoelectron is produced in the interaction of an X-ray with the detector material. A K X-ray of ~25 keV and mean free path of ~85 μm may also be produced in this interaction. The photoelectron loses energy by ionization, creating electron-hole pairs along its path. The range of the photoelectron depends on the energy of the interaction. For example, a 40 keV photoelectron has a range of ~10 μm, whereas the range is ~47 μm for a 100 keV photoelectron.[11] Since electron-hole production increases towards the end of the track, the clouds are not uniform in charge density. For a 100 keV photoelectron, 30% of the electron-hole pairs are created in the last 7μm of its track.

Moreover, the electrons released along the photoelectron track diffuse while drifting to the electrodes, forming an expanding charge cloud. The change in electron concentration M of the cloud as a function of time and position can be described by the solution of Fick's equation,[12]

$$\mathrm{M} = \frac{\mathrm{M_o}}{2\,(\pi\,\mathrm{D\,t})^{1/2}}\ \exp\left[\frac{-\mathrm{x}^2}{4\,\mathrm{D\,t}}\right] \qquad (1)$$

where $\mathrm{M_o}$ is the initial concentration and D is the diffusivity, which is $\sim\,26\,\mathrm{cm^2/s}$ for electrons in CZT at room temperature. The time between interaction and collection, t, decreases linearly with depth of interaction from the top of the detector, and thus the size of the cloud decreases as depth of interaction increases, as shown in Fig. 3.

3. MEASUREMENTS

We used collimated X-rays from a ^{57}Co rradioactive source to study the detector response. This source has a dominant line at 122 keV, and two weaker lines at 136 keV and 14.4 keV. The collimator uses a stack of precision, laser machined tantalum disks with holes ranging from 30 to 60 μm to form a 3 mm thick layer with a fine hole passing through it.[2] The hole is tapered to give a uniform X-ray intensity in its 30 μm aperture. This was placed ~0.5 mm from the detector and the radioactive source was ~10 cm from the aperture. The position of the collimator was controlled by an X-Y stage with 10 μm precision.

The signals from two adjacent anodes, the steering electrode and a cathode were processed by shaping, amplifying and triggering circuits, and digitized by ADC's to give the total signal on each electrode. An on-line program processed the data and built multiple spectra according to various event selection criteria.[3,13] If the signal on any electrode exceeded its threshold, the system was triggered and all pulse heights were measured and recorded to build event lists.

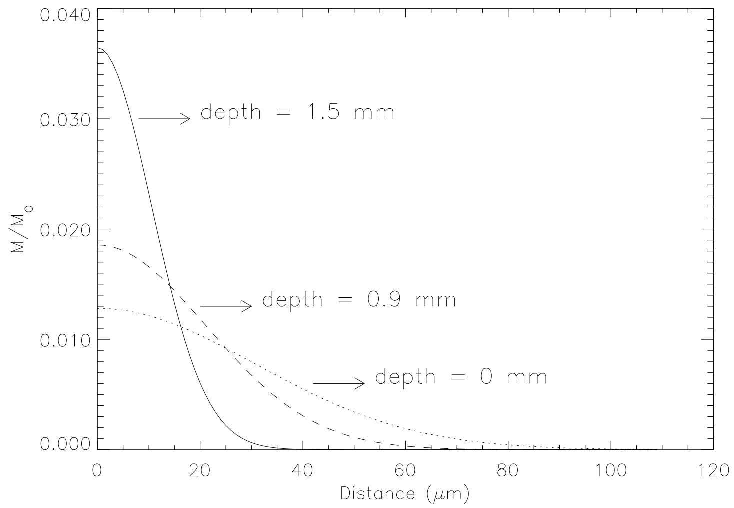

Figure 3. Concentration of particles as a function of position for different interaction depths. Profiles show the concentration when the electrons have drifted to a depth of 1.7 mm. M_o is the initial concentration. From Kalemci et al.[6]

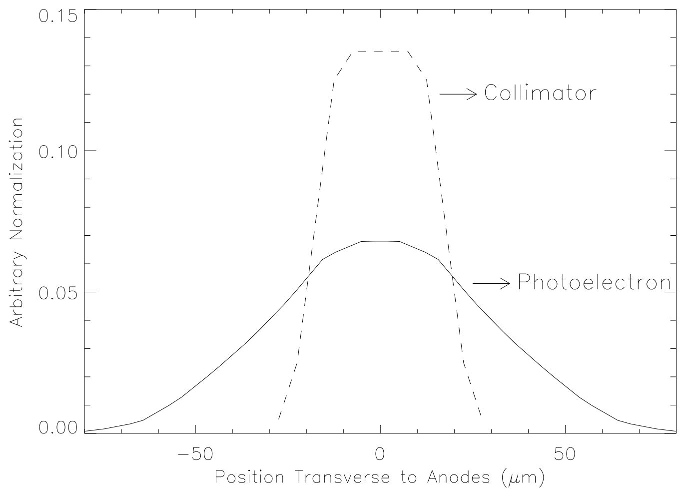

Figure 4. The dashed line (Collimator) shows the lateral distribution of interaction positions with respect to collimator position. The solid line (Photoelectron) corresponds to the lateral distribution of endpoints of photoelectron tracks. From Kalemci et al.[6]

We scanned perpendicular to the anode strips with the 30 μm collimator. The position with an equal number of counts at each anode was assumed to correspond to the center of the steering electrode. Other positions were measured with respect to this point. The illumination point was kept centered on a cathode strip.

We obtained the distribution of electron clouds for a given collimator position in two steps. First, we calculated the flux of photons from the collimator to get the lateral distribution of interaction positions. Then, we convolved this distribution with the photoelectron path distribution. Fig. 4 shows the distribution of end points of photoelectron tracks along with the distribution of initial positions of interactions.

Since 122 keV X-rays interact throughout the detector, we were able to study the dependence of charge splitting on interaction depth. It is well known that the cathode signal decreases as depth of interaction increases, and the ratio of cathode signals to anode signals indicates the interaction depth.[1,8] We sorted events into depth ranges according to their cathode to anode ratios. Then, using the photoelectric absorption coefficient of CdZnTe for 122

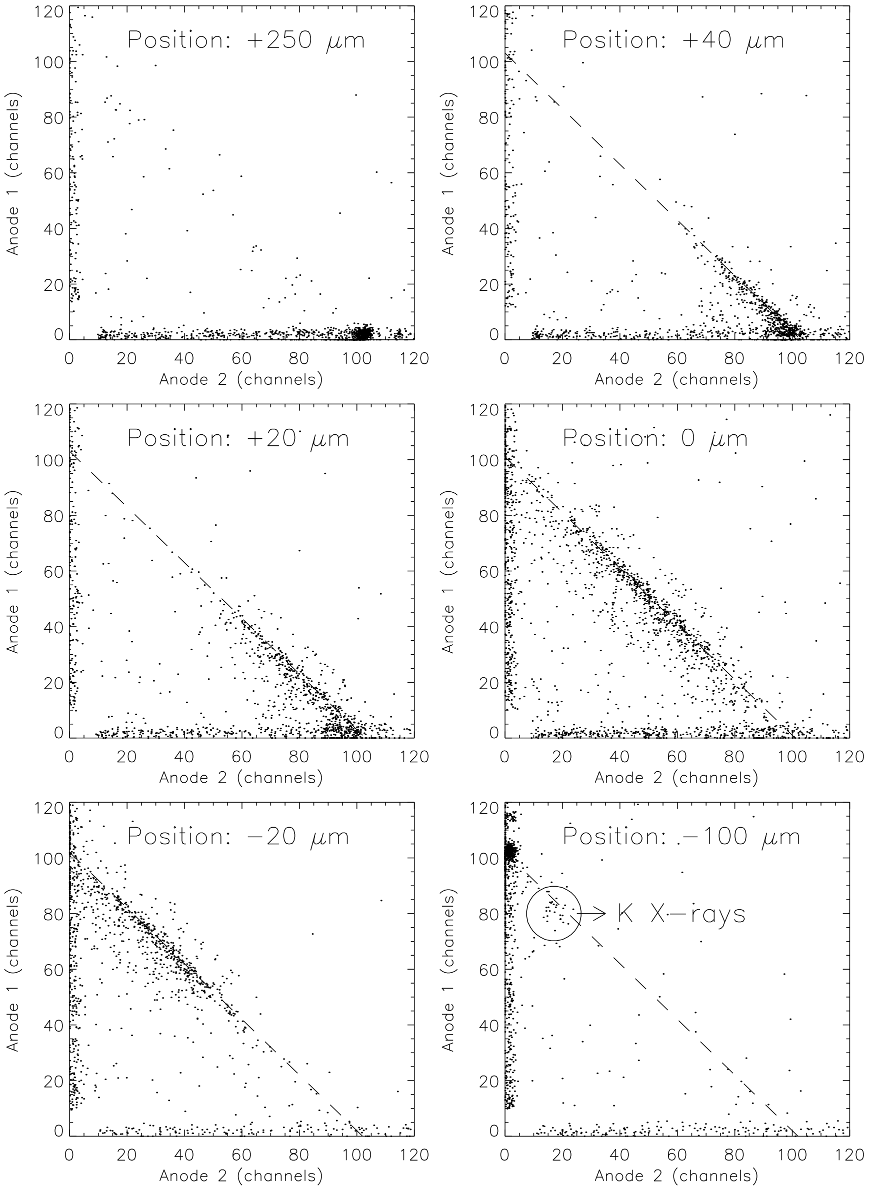

Figure 5. Scatter plots of anode signals. Each point represents one event. The positions are the distance of the collimator from the center of the steering electrode (which is denoted by Position: $0\,\mu$m). The dashed lines represent the ideal case where all charges are collected by the two anodes. $100\,\mu$m away from the steering electrode, K X-rays interacting on neighbor anodes appear as a separate feature. From Kalemci et al.[6]

keV photons and the number of counts in each range, we calculated the boundaries of the depth ranges.

4. RESULTS AND INTERPRETATIONS

4.1. Charge splitting

The relative signals on the two neighbor anodes were found to be a strong function of beam position, as shown in Fig. 5. At $+250\,\mu$m, above the center of anode 2, there is negligible charge splitting. All 122 keV (channel $\sim$100) and

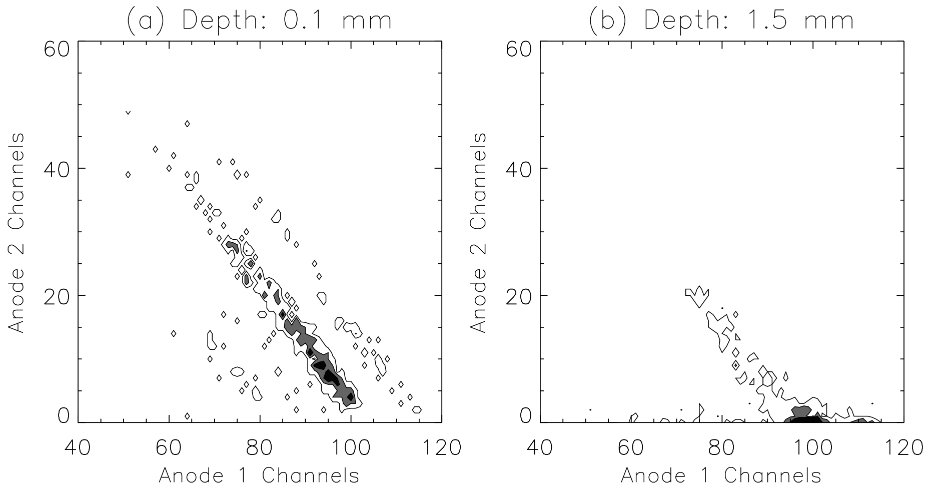

Figure 6. The depth dependence of charge splitting. Figures are contour plots of 2D histograms of Anode 1 versus Anode 2 signals. Darker regions indicate higher density of points. The collimator is at $-40\,\mu$m. Panels (a) and (b) correspond to average depths of 0.1 mm and 1.5 mm, respectively. From Kalemci et al.[6]

136 keV (channel ~113) interactions are collected at the anode. The remaining continuum is background, except at channel ~12 (14.4 keV) where another line of ^{57}Co falls. Except for K X-rays interacting on neighbor anodes, no splitting occurred for all positions greater than $100\,\mu$m from the steering electrode center. For collimator positions less than $100\,\mu$m from the steering electrode, some events fall on a diagonal line representing full energy in the summed anode signals (x+y=122 keV). At position $0\,\mu$m, three such lines (136 keV, 122 keV and ~97 keV escape peak) can be observed. Negative positions mean the collimator is near Anode 1, so most charge is collected by it, as indicated in the $-20\,\mu$m and $-100\,\mu$m panels. Since the points lie on a diagonal line, little charge is lost to the steering electrode or the gap.

4.2. Effects of diffusion and photoelectron range

Charge splitting is expected to be greater for interactions near the cathode, since the cloud must drift for a greater distance which results in more diffusion. In Fig. 6, we showed this to be the case by comparing the sharing effects at the top and the bottom of the detector for a collimator position $40\,\mu$m away from the center of the steering electrode. Panel (a) is for interactions in the top 0.2 mm of the detector and significant charge splitting occurs. However, most of the interactions at the bottom of the detector are fully collected at anode 1, as shown in panel (b).

We tested our model by comparing the predicted onset of charge splitting versus the beam position at which the charge splitting was observed. The former was calculated using the photoelectron range distribution (Fig. 4) and the predicted broadening due to diffusion (Eq.(2) and Fig. 3). We defined the onset of charge splitting for each depth as the collimator position at which the neighbor anode received more than 5% of the signal for at least 5% of all the events.[6] For 5% of all interactions, the photoelectron range is greater than $45\,\mu$m as determined by integrating the solid curve in Fig. 4. By using the diffusion formula, we predicted the distance beyond which 5% of the electrons reside, and called it L(5%). Then the sharing onset is expected to occur at $45\,\mu$m + L(5%). This distance was calculated for three depths and compared with measurements, with the results shown in Table. 1.

Average depths, depth ranges, L(5%) values, and predicted onsets are shown in the first four columns of Table 1. The collimator positions where the onsets were observed and the nearest positions where no sharing were observed are shown in the last two columns. Uncertainties in the observations correspond to the positioning of the collimator, and uncertainties in the calculations were combinations of various effects such as sampling preferentially lower depths within one depth range, uncertainty of charge sharing due to K X-ray interactions, and our assumption that the initial concentration of the electron cloud is a delta function. The results showed that observational onsets were within the uncertainties of the estimated onsets.

Table 1. Predicted and observed onset of charge sharing

Avg. Depth	Depth Range	L(5%)	Predicted	Observed	No sharing
0.1 mm	0 - 0.2 mm	$50^{+1}_{-0}\,\mu$m	$95^{+1}_{-10}\,\mu$m	$95 \pm 5\,\mu$m	$105 \pm 5\,\mu$m
0.44 mm	0.35 - 0.53 mm	$43^{+2}_{-0}\,\mu$m	$88^{+2}_{-10}\,\mu$m	$80 \pm 5\,\mu$m	$100 \pm 5\,\mu$m
1.1 mm	0.9 - 1.3 mm	$30^{+4}_{-0}\,\mu$m	$75^{+4}_{-10}\,\mu$m	$65 \pm 5\,\mu$m	$85 \pm 5\,\mu$m

4.3. Charge loss to the steering electrode and gaps

For interactions within $\pm 60\,\mu$m of the steering electrode the summed anode signal is reduced by a few percent and shows tailing. However, a simulation neglecting diffusion and photoelectron range predicts that electrons from these events would drift only to the steering electrodes, producing no signal on the anodes and full signal on steering electrode. We showed[6] that, for some of the interactions, the steering electrode has positive signals but not the full signal, which means that it collects electrons for some events but not all. These apparently discordant results could be reconciled if the number of field lines ending at the steering electrode is smaller than predicted by the model and/or the electron cloud is larger than $\sim 100\,\mu$m. Then only a fraction of the electrons would be collected by it, which could explain the lack of full energy signals on the steering electrode.

It is difficult to interpret the steering electrode pulses to study such effects. The steering electrode has extended weighting potentials and therefore, for most of the events, the trapped holes induce a large negative signal. On the other hand, only a small fraction of electrons induce positive signal, making the overall signal negative. (See Kalemci et al.[1] for weighting potential calculations.) Therefore, we analyzed summed anode spectra, since anode signals do not suffer significantly from hole trapping, due to the small pixel effect.

We compared the summed anode spectrum for a collimator position above Anode 2, where there is no charge loss, with that of above the steering electrode where cahrge loss is a maximum. This analysis was done for various depth ranges and the results are shown in Fig. 7. At each depth we considered the shift of line centroid over the steering electrode relative to that over the anode. Near the top of the detector (0.1 mm), the shift is $\sim$1%. For deeper interactions, the shift was larger. For the average depth of 1.5 mm, the centroid shifted $\sim$9%. The increase of centroid shift with increasing depth is consistent with the diffusion of electron cloud with time. Because the electrons have less time to diffuse for deeper interactions, the charge cloud is smaller and the steering electrode collects more of the electrons.

We estimated the size of the detector region where the field lines end at the steering electrode by calculating the lateral extent of the part of the charge cloud which drifts to the steering electrode. At the depth range, 1.1 mm to 1.7 mm, the maximum charge lost is $\sim$15% (Fig 10d). Assuming these events occurred at 1.7 mm, and the photoelectrons moved towards the steering electrode with no additional broadening, a diffusion time of t=40 ns results in 15% of the electrons being within $\pm 2\,\mu$m of the charge cloud's center. Thus, the region with field lines ending on the steering electrode measures just $\pm 2\,\mu$m. However, our electric field calculation (Fig. 2) predicted a $\pm 20\,\mu$m region. This would result in the majority of electrons being collected by the steering electrode for interactions above it at any depth. We therefore concluded that the model overestimates the number of field lines ending at the steering electrode.[6]

5. CONCLUSIONS AND FUTURE DIRECTIONS

Diffusion is a very important mechanism causing charge splitting. For an interaction with minimal depth in the detector, the electron cloud size increases to $\sim 100\,\mu$m due to diffusion while it drifts 2 mm to the anodes in a $\sim$1000 V/cm field. The solution of Fick's equation predicts that the size of the cloud is a function of depth. We tested this by mapping the onset of charge sharing as a function of interaction depth. The results were in good agreement with the calculated onsets. Another important mechanism affecting charge sharing is the photoelectron range. W ithout considering its effects, the predicted onsets in Table 1 would be reduced by $\sim 20\,\mu$m, contrary to the observed onsets.[6]

Our calculation of electric field lines predicts that interactions above the steering electrode would have the majority of their electrons collected by the steering electrode, but the laboratory tests indicate that this is not the

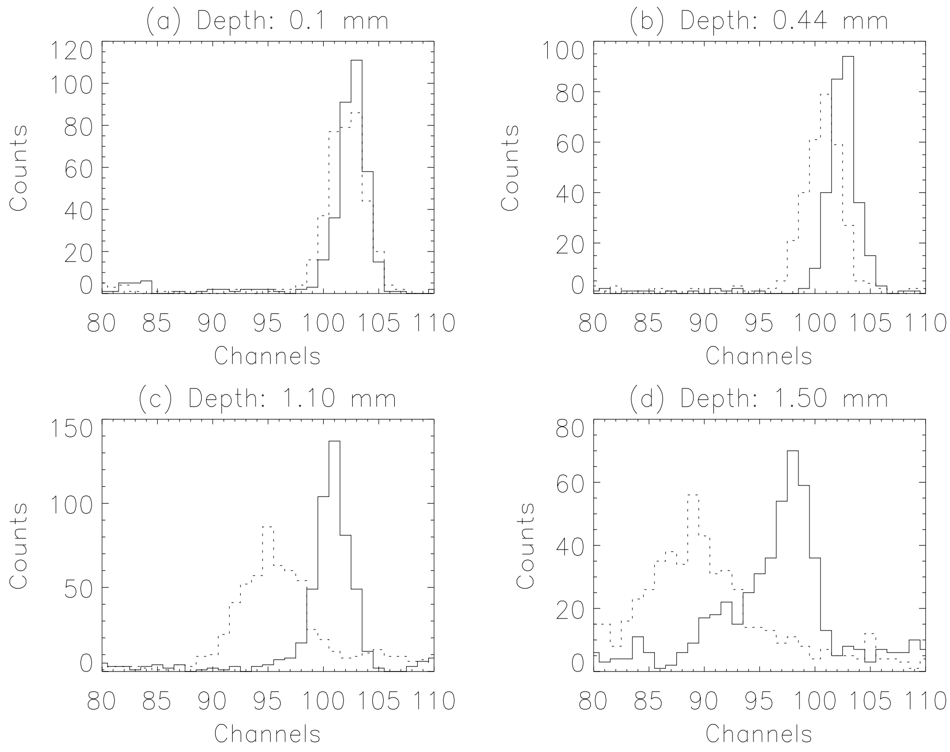

Figure 7. Depth dependence of signal lost to the steering electrode. Each panel contains two anode spectra, one for collimator directly above one anode (solid line) and other directly above the steering electrode (sum of two anodes). These show that as the interactions get deeper the steering electrode collects more charge, reducing the summed anode signal. From Kalemci et al.[6]

case. Rather, ∼90% of the electrons reach the anodes for interactions only 0.5 mm above the steering electrode. This implies that the simulation overestimates the number of field lines ending at the steering electrode. A similar effect was reported in a study by Prettyman et al.[10] where they discussed possible causes, such as band bending near the anodes, surface effects, and microscopic defects.

In the region where charge splitting occurred, the summed anode spectrum peaks in Fig. 7 signal were 89% to 99% of those for single anode events. These deficits represent electrons lost to the steering electrode and the gaps.[6] These effects can be corrected. First, the ratio of cathode-to-anode signals can be used to infer the depth, allowing a depth-dependent correction for hole trapping as shown by Kalemci et al.[1] Second, for shared events, the ratio of the signals on the two anodes indicates the transverse position which can be used, along with the depth, to correct for the signal lost to the steering electrode and the gaps. Such a full correction is the subject of future work.

ACKNOWLEDGMENTS

This work was supported by NASA SR&T Grant NAG5-5111 and NASA Grant NAG5-8498. Technical support was provided at UCSD by Fred Duttweiler, George Huszar, Charles James, Phillippe Leblanc, David Malmberg, Ron Quillan and Ed Stephan. Authors would like to thank Richard Rothschild, William Heindl, John Tomsick and Tom Skelton for their valuable discussions. We also would like to thank Kimberly Slavis at WU for her contributions. Emrah Kalemci was partially supported by TUBITAK.

REFERENCES

1. E. Kalemci, J. L. Matteson, R. T. Skelton, P. L. Hink, and K. R. Slavis, "Model calculations of the response of CZT strip detectors," in *Hard X-Ray, Gamma-Ray, and Neutron Detector Physics*, R. B. James and R. C. Schirato, eds., *Proc. SPIE* **3768**, pp. 360–373, 1999.

2. J. L. Matteson, W. Coburn, F. Duttweiler, T. Gasaway, W. A. Heindl, P. C. Leblanc, D. R. MacDonald, M. R. Pelling, L. E. Peterson, R. E. Rothschild, R. T. Skelton, P. Hink, and C. Crabtree, "CdZnTe strip detectors for high-energy x-ray astronomy," in *Hard X-Ray / Gamma-Ray and Neutron Optics, Sensors, and Applications*, R. B. Hoover and F. P. Doty, eds., *Proc. SPIE* **2859**, pp. 58–73, 1996.
3. J. L. Matteson, D. E. Gruber, W. A. Heindl, M. R. Pelling, L. E. Peterson, R. E. Rothschild, R. T. Skelton, P. Hink, K. R. Slavis, and W. R. Binns, "High energy X-ray imaging spectrometer - HEXIS," in *EUV, X-Ray, and Gamma-Ray Instrumentation for Astronomy IX*, *Proc. SPIE* **3445**, pp. 445–457, 1998.
4. S. Ramo, "Currents induced by electron motion," *Proc. I.R.E.* **27**, pp. 584–585, 1939.
5. MAXWELL, *3D Field Simulator*, Ansoft Corporation, Four Station Square, Suite 660, Pittsburgh, PA 15219-1119 USA, www.Ansoft.com.
6. E. Kalemci and J. L. Matteson, "Investigation of charge sharing among electrode strips for a CdZnTe detector," *NIM A* **submitted**, 2000.
7. Y. F. Du, Z. He, W. Li, and G. F. Knoll, "Monte Carlo investigation of the charge sharing effects in 3-D position sensitive CdZnTe gamma ray spectrometers," *IEEE Trans. on Nucl. Sci.* **46, 4**, pp. 844–847, 1998.
8. Z. He, W. Li, G. F. Knoll, D. K. Wehe, and Y. F. Du, "Effects of charge sharing in 3-D position sensitive CdZnTe gamma-ray spectrometers," *Nucl. Instr. and Meth. A* **439**, pp. 619–624, 2000.
9. A. E. Bolotnikov, W. R. Cook, F. A. Harrison, A. S. Wong, S. M. Schindler, and A. C. Eichelberger, "Charge loss between contacts of CdZnTe pixel detectors," *Nucl. Instr. and Meth. A* **432**, pp. 326–331, 1999.
10. T. H. Prettyman, M. K. Smith, P. N. Luke, M. Amman, and J. Lee, "Investigation of charge collection in multi-electrode CdZnTe detectors," in *Hard X-Ray, Gamma-Ray, and Neutron Detector Physics*, R. B. James and R. C. Schirato, eds., *Proc. SPIE* **3768**, pp. 27–36, 1999.
11. NIST, *Physical Reference Data*, ESTAR, http://physics.nist.gov/PhysRefData/Star/Text/ESTAR.htm.
12. W. R. Beam, *Electronics of Solids*, Mc-Graw Hill Book Co., New York, 1965.
13. K. Slavis, P. Dowkontt, F. Duttweiler, J. Epstein, P. L. Hink, G. L. Huszar, P. Leblanc, J. L. Matteson, R. T. Skelton, and E. Stephan, "High altitude balloon flight of CdZnTe detectors for high energy X-ray astronomy," in *EUV, X-Ray, and Gamma-Ray Instrumentation for Astronomy IX*, *Proc. SPIE* **3445**, pp. 169–184, 1998.